

Excitonic structure of bulk AlN from optical reflectivity and cathodoluminescence measurements

E. Silveira,* J. A. Freitas, Jr., and O. J. Glembocki
Naval Research Laboratory, ESTD, Washington, DC 20375-5347, USA

G. A. Slack and L. J. Schowalter
Crystal IS, Inc., Latham, New York 12110, USA
 (Received 27 September 2004; published 7 January 2005)

Reflection measurements in the near-band-edge region of bulk AlN crystals have been performed as a function of temperature. The optical reflectance spectra of an *a*-face AlN sample show a feature at about 6.029 eV, which we assign to the free exciton *A*. The observation of the free exciton *A* first excited state yields the estimated values of the direct band gap and the limit of the electron effective mass. Optical reflectance measurements performed on AlN samples with two different crystallographic orientations allow the observation of transitions associated with the optical selection rules related to the so-called *A*, *B*, and *C* excitons. It was not possible to fully resolve the *B*- and *C*-excitonic transitions, which were observed at about 6.243 and 6.268 eV, respectively. Using the measured exciton energies and a quasicubic model developed for the wurzite crystal structure we estimate the spin-orbit splitting $\delta=36$ meV and the crystal-field splitting $\Delta=-225$ meV.

DOI: 10.1103/PhysRevB.71.041201

PACS number(s): 78.40.Fy, 71.70.Ch, 71.70.Ej, 71.22.+i

I. INTRODUCTION

The combination of important physical properties of group III-nitride-based semiconductors has prompted rapid research progress and the commercial availability of optoelectronic devices in the past decade. They are being used for high-density optical data storage, high power and high-temperature applications, solid-state lighting, and solar-blind detectors, among other applications.¹ At the present time the active layers of these devices, despite the relatively high efficiency, are not fabricated on a substrate that is really suitable for their epitaxy, such as sapphire and SiC. More recently there has been a continuing effort to further improve the quality and availability of ultralow dislocations density native hexagonal (wurzite-type) AlN substrates, which have the potential to enable critical advances in multiple III-nitride device technologies. Despite the increasing importance of AlN, key questions about its very basic physical properties remain unsolved or controversial in the literature.

In the band structure of the direct gap wurzite-type AlN the degeneracy of the *p*-like valence bands at the Γ point is lifted by both noncubic crystal-field splitting and spin-orbit splitting, resulting in three valence bands at the center of the Brillouin zone. This splitting of the valence bands results in three interband transitions to the lowest conduction band, referred to as *A*, *B*, and *C* in order of increasing transition energy. The theoretical predictions about the spin-orbit splitting and the negative crystal-field splitting, and their influences on the electronic properties of AlN, have to be confirmed experimentally. As part of this effort optical spectroscopy is a very useful technique in order to elucidate questions about the AlN band structure and excitonic features.

The majority of the studies on the near-band-edge (NBE) UV emission of wurzite-type AlN are reports on films heteroepitaxially grown on SiC, sapphire, or Si substrates.²⁻¹⁰ An even smaller number of studies deal with bulk AlN.¹¹⁻¹⁵ In the present work we report on optical reflectivity (OR)

experiments of high quality, large, bulk AlN single crystals with different crystallographic orientations. The results taken at different sample temperatures will be compared to cathodoluminescence measurements conducted in our group.¹³⁻¹⁵ Important parameters like crystal-field splitting and spin-orbit splitting were obtained based on our reflectivity results.

II. EXPERIMENTAL DETAILS

The large, bulk AlN single crystals used in this experiment were grown by a self-seeded sublimation-recondensation technique. Both *c*-face (0001) and *a*-face (11 $\bar{2}$ 0) single-crystal wafers of AlN, obtained by cutting and polishing the crystals, were investigated. X-ray diffraction measurements attested to the crystalline quality of the samples. The *a*-face, OR sample is sample 00G of Ref. 12. The *c*-face, cathodoluminescence (CL) sample consisted of a homoepitaxial ~ 0.5 μm -thick film grown by organometallic vapor phase epitaxy on the Al face of a 287- μm -thick AlN, *c*-axis substrate. The *c*-axis vector is tilted 10° from the surface-normal, sample AFE. More details on the growth and structural characterization can be found elsewhere.^{12,14,16,17} CL measurements were carried out using a commercial electron gun, installed in an ultrahigh vacuum chamber, in order to excite the samples. Electron-beam currents between 1 and 5 μA and energies between 5 and 15 keV were typically used. The light emitted by the samples, collected and focused by a set of parabolic mirrors, was dispersed by a 0.85-m double spectrometer equipped with 1200 groves/mm gratings. The dispersed light was subsequently detected by an UV-sensitive GaAs photomultiplier connected to a computer-controlled photon counter.

For the optical reflectance measurements a 150-W deuterium lamp was used as the light source, after being dispersed by a 0.5-m monochromator equipped with a 1200 groves/mm grating. The sample was placed inside a cold-finger cryostat and the light reflected by the sample was then

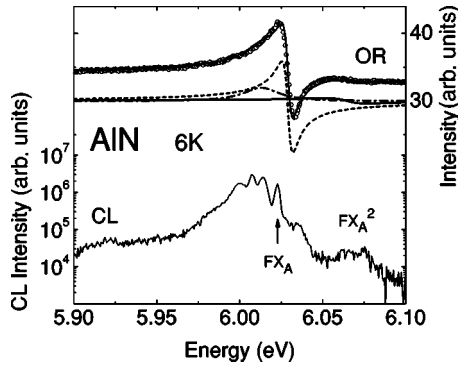


FIG. 1. OR shows the optical reflectivity spectrum of the *a*-face AlN sample and CL the cathodoluminescence spectrum of a *c*-face homoepitaxial AlN film. The full curve in the upper part represents our best fit to the experimental data (hollow symbols). The three curves composing the full OR curve are shown separately and vertically displaced.

detected by a solar-blind photomultiplier linked to a photon counter system. The whole light path was purged with nitrogen gas in order to minimize absorption by the oxygen molecules present in the air. The incident beam impinged on the sample at an angle of about 20° from the wafer surface normal.

III. EXPERIMENTAL RESULTS AND DISCUSSION

Figure 1 depicts typical low-temperature CL (bottom) and reflectance (top) spectra in the NBE region for the *a*-faced sample. In the CL spectrum several transitions are clearly observed, and these have been tentatively assigned to free and bound exciton recombination processes based on thermal quenching studies.¹⁵ In the CL data the free exciton *A* (FEA) is observed at about 6.023 eV and another feature at about 6.036 eV, which was then attributed to another free exciton, due to its intensity versus temperature behavior. The spectrum also shows a structure at about 6.07 eV named as FX_A^2 and is attributed to the excited states of the FEA by comparison with similar structure in the PL spectra of GaN.¹⁵ Figure 1 shows, in its upper part, a representative optical reflectance spectrum measured over the same energy region covered by the CL spectrum. Both measurements were taken at 6 K and no modulation of any kind was used. The observed line shape in the optical reflectance spectrum is typical for an excitonic transition. The excitonic effects are known to enhance the oscillator strength at the band gap and to significantly sharpen line shapes. The excitonic transitions in the reflectivity data were fitted to a Lorentzian dielectric function given by

$$\varepsilon(E) = 1 + \sum_j \left[\frac{A_j \exp(i\phi)}{(E - E_{X_j} + i\Gamma_j)} \right], \quad (1)$$

where E is the photon energy, E_{X_j} the transition energy for the j th excitonic state, and Γ_j the lifetime broadening factor of that state. A_j is the oscillator strength for the j th transition and contains transition matrix elements, and ϕ is a phase factor to account for optical interference effects caused by effects such as dead layers.

It is important to note that the line shape of the reflectance data of Fig. 1 is asymmetric with more oscillator strength in its lower energy portion between 6.00 and 6.025 eV. In addition a weak feature is clearly visible near 6.05 eV. A fit to the data of Fig. 1 with a single excitonic transition using Eq. (1) significantly underestimated the oscillator strength in the lower energy portions of the line shape and could not account for additional structure near 6.05 eV. In order to reproduce the reflectance data we employed three transitions. The result of the fit to the real part of Eq. (1) is shown in Fig. 1 as a solid line through the data. The line shapes of the three individual components are plotted below the data. The main excitonic line in the OR occurs at 6.029 eV and is accompanied by a satellite transition at 6.065 eV. Their line shape fits well to the real part of Eq. (1) and has the expected line shape of excitonic transitions. The transition energies from the reflectance of the *a* face agree well with peaks in the CL data from the *c* face that have been attributed to the $n=1$ and $n=2$ states of the free exciton as mentioned above. Interestingly, the ratio of the two integrated intensities for the reflectance lines at 6.029 and 6.065 eV obtained from the fit is 5, which is in reasonable agreement with the expected ratio of 8 for the $n=1$ and $n=2$ excitonic transitions.

In addition to the free exciton, the reflectance data show some increased oscillator strength below the excitonic transitions that has been attributed to impurity related absorption. In this case, the line shape is characteristic of the imaginary part of Eq. (1). This type of behavior has previously been observed in the reflectance of very thin AlGaIn films grown on GaN. Because of the weak absorption from the very thin AlGaIn film, Jiang *et al.*¹⁸ have shown that the reflectance of that film was characteristic of a double pass absorption measurement and that the line shape was best represented by the imaginary part of Eq. (1). Our reflectance data below the free exciton energy shows a similar line shape at an energy of 6.013 eV and this can be attributed to impurity related transitions in the AlN that are also observed in *c*-face CL near 6.014 eV (see also Ref. 15). The line shape indicates that the impurity related transitions are very weak and the reflectance measurement is a “double pass” absorption with light passing through the wafer and reflecting from the back surface. It is important to note that impurity related transitions in modulated reflectivity have been observed by Shanabrook *et al.*¹⁹ in GaAs quantum wells and confirmed through photoluminescence. Their experiments also observed a similar line shape.

From the energy values for the FEA and its first excited state in the OR data we estimate the free exciton *A* binding energy as 48 meV from an extrapolation to $n=\infty$, which gives an estimated energy gap of 6.077 eV at 6 K for AlN. This result is a little smaller but in relatively good agreement with previously reported values for the band-gap energy of AlN obtained in heteroepitaxial films¹⁰ for light polarized perpendicular to the *c* axis.

Moore *et al.*²⁰ found the low-frequency birefringence of AlN to be very high. They determined the ordinary static dielectric constant as 7.76 and the extraordinary as 9.32 for AlN. The reduced effective mass for the free exciton is determined assuming a hydrogenic expression for the free exciton binding energy. Taking the two values mentioned²⁰ for

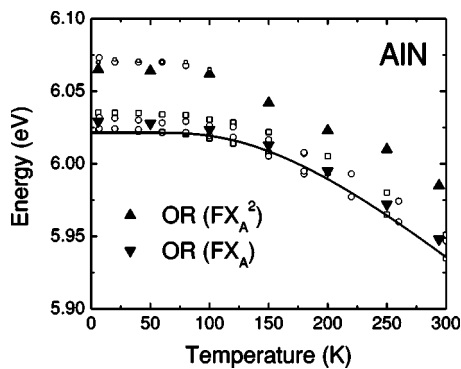


FIG. 2. Energy positions of the excitonic features as a function of temperature. The filled symbols depict the optical reflectivity data and the hollow ones the CL data. The full line represents the Bose-Einstein relation for the energy as a function of the temperature.

the dielectric constant as the limits, the effective mass for the free exciton ranges from 0.211 to $0.305m_0$. Based on measurements of the Mg acceptor binding energy in doped AlN epilayers,⁹ the effective-mass theory, and the dielectric constant values mentioned earlier, the average hole effective mass in AlN was estimated between 2.26 and $3.26m_0$. In our case it is possible to estimate the electron effective mass by using these hole effective mass extreme values and the exciton effective mass limits calculated above. We estimate the electron effective mass in AlN spanning from 0.233 to $0.336m_0$. These values are in very good agreement with our previous results for the electron effective mass derived from CL measurements.¹⁴

Optical reflectance spectra of the *a*-face AlN sample 00G were also taken as a function of temperature. Using the same procedure described above all the excitonic features in the optical reflectance spectra have been fitted assuming the same number of oscillators at all temperatures. The results are summarized in Fig. 2. In this figure the energy positions of the two observed oscillators in the optical reflectance spectra are presented as a function of temperature by the full symbols. The hollow symbols are the peak positions observed in CL measurements and have been presented elsewhere.^{14,15} Interestingly there is very good correspondence between the CL and reflectivity results over a broad range of temperatures.

An empirical description of the band-gap variation for polar semiconductors with the optical and acoustical-phonon branches energetically close was obtained in the past assuming Bose-Einstein statistics.²¹ The full lines represent the Bose-Einstein fitting for the temperature variation of the band gap. For these curves we used the same parameters as for the description of our CL measurements on an AlN homoepitaxial film.^{14,15} It is possible to observe that the optical reflectance data fits very well into this model with the same parameters as the ones used for the CL measurements.

Reported theoretical calculations generally agree that in wurzite-type AlN the crystal-field splitting is negative, in contrast to a positive value for GaN. In order to study the influence of the negative crystal-field splitting on the optical properties of AlN and consequently on the selection rules for

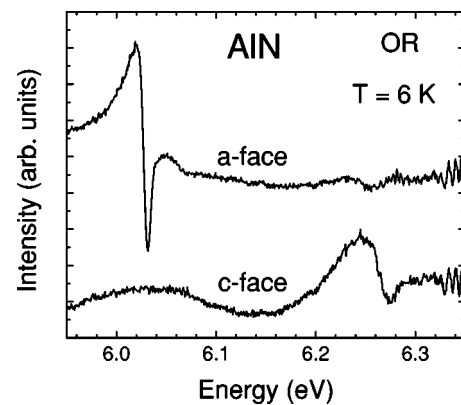


FIG. 3. Low-temperature optical reflectivity data at near-normal incidence for AlN samples oriented in two different crystallographic orientations.

its optical transitions, we conducted optical reflectance experiments on two samples with different crystallographic orientations. Figure 3 shows two optical reflectance spectra taken from the AlN sample number 00G with *a*-face (upper curve) and *c*-face sample number ACE.3 (lower curve) acquired at 6 K. The *a* axis was within $\pm 2^\circ$ of the surface normal for sample 00G; the *c* axis was tilted 6° away from the normal for sample ACE.3. The spectra were displaced vertically for a better visualization. We observe that in the *a*-face AlN spectrum has two distinct regions with excitonic features: One not resolved and more pronounced at about 6.029 eV, and a much less intense feature at about 6.243 eV. The energy region in the vicinity of 6.25 eV was fit to two Lorentzian oscillators for both samples, representing the *B* and *C* excitons. From the fit we find that the *B* and *C*-excitonic transitions occur at 6.243 and 6.268 eV, respectively. In the *c*-face AlN spectrum *B* and *C* excitons are easily observed, while for the *a*-face sample the *B* exciton dominates the energy region around 6.25 eV. According to their energy positions and selection rules we can attribute the line at 6.029 eV to the *A* exciton and the lines at 6.243 and 6.268 eV to *B* and *C* excitons, respectively. The *B* and *C* excitons were well described by two oscillators, in agreement with the expected number of transitions and band-structure calculations. Calculated dipole transition matrix elements between the conduction state and the three valence states at the Γ point of the Brillouin zone for wurzite-type AlN show that for light polarized parallel to the *c* axis, as is the case in our spectrum for the *a*-face sample, only one transition is allowed, i.e., only the *A* exciton is expected. The appearance of a much less intense feature observed at 6.243 eV (*B* exciton) in the *a*-face sample may be due to the fact that the incident light was not exactly perpendicular to the sample surface. For light polarized perpendicular to the *c* axis both the *B*- and *C*-excitonic transitions are allowed,¹⁰ as is the case observed for the *c*-face sample.

Note that the peak at about 6.036 eV in the *c*-face CL spectrum was previously assigned to recombination processes involving the annihilation of FEB based on temperature quenching studies.^{14,15} However, the reflectance results discussed in the present manuscript on a different *c*-face sample do not support this model. Currently, detailed CL

studies of samples with different crystallographic orientations are planned in order to investigate further the nature of this CL spectral feature.

Hopfield's quasicubic model²² for wurzite crystals for the relation between the excitons energies is described by the following equations observing their symmetry:

$$E_{A,C} = E_B + \frac{\delta + \Delta}{2} \pm \sqrt{\left[\left(\frac{\delta + \Delta}{2}\right)^2 - \frac{2}{3}\delta\Delta\right]}, \quad (2)$$

where $E_{A,B,C}$ are the energies for the A , B , or C excitons, respectively.

Hopfield, in his paper,²² estimates the error in the quasicubic model spin-orbit interaction as probably of order (Δ/E_g) . As pointed out earlier, we estimated E_g for AlN to be about 6.077 eV. We evaluated the crystal-field and spin-orbit splitting from Eq. (2) by taking the energy for the A exciton to be 6.029 eV and the above-mentioned energies of 6.243 and 6.268 eV for the B and C excitons, respectively. In addition, due to the lack of data for the binding energies of the B and C excitons, and based on the results for GaN where the A , B , and C excitons have binding energies that differ by only a few meV,²³ we assumed that all of the excitons had the same binding energy. With this, we determined the spin-orbit splitting $\delta=36$ meV and the crystal-field splitting $\Delta=-225$ meV. Although there is a lack of experimental values for these two parameters for AlN, they have been determined theoretically by several authors. The crystal-field splitting Δ , in particular, showed a strong dependency on variation in the

lattice parameters a , c , and u . Suzuki *et al.*,²⁴ using a self-consistent full-potential LAPW method, reported a value of 58 meV for Δ , and Li *et al.*,¹⁰ using the local-density approximation, calculated a value of -219 meV for Δ and 13 for δ , while da Silva and Persson,²⁵ using the local-density approximation, reported $\Delta=-212$ meV and $\delta=13.2$ meV. Our results are in good agreement with the later theoretical work.

IV. CONCLUSIONS

The optical properties of wurzite-type bulk AlN crystals have been investigated using low-temperature optical reflectance in the near-band-edge region of the spectrum. Since we observe the free exciton A and its first excited state we estimate the band gap to be 6.077 eV for wurzite AlN. The temperature dependence of the AlN A -exciton double structure follows the empirical model assuming Bose-Einstein statistics for the description of the energy band gap. Based on a quasicubic model developed for the wurzite crystal, and on the experimental exciton energy values, it was possible to determine for AlN the spin-orbit splitting $\delta=36$ meV and the crystal-field splitting $\Delta=-225$ meV.

ACKNOWLEDGMENTS

The authors would like to thank B. V. Shanabrook for helpful comments. The work at NRL was partially supported by the ONR-IFO and ONR, monitored by C. E. C. Wood.

*Permanent address: Depto. de Física, UFPR, CP 19044, Curitiba-PR, Brazil.

¹H. Morkoç, *Nitride Semiconductors and Devices* (Springer, Heidelberg, 1999).

²C.-M. Zetterling, M. Östling, K. Wongchotigul, M. G. Spencer, X. Tang, C. I. Harris, N. Nordell, and S. S. Wong, *J. Appl. Phys.* **82**, 2990 (1997).

³X. Tang, F. Hossain, K. Wongchotigul, and M. G. Spencer, *Appl. Phys. Lett.* **72**, 1501 (1998).

⁴Y. Shishkin, R. P. Devaty, W. J. Choyke, F. Yun, T. King, and H. Morkoç, *Phys. Status Solidi A* **188**, 591 (2001).

⁵N. Teofilov, K. Thonke, R. Sauer, D. G. Ebling, L. Kirste, and K. W. Benz, *Diamond Relat. Mater.* **10**, 1300 (2001).

⁶T. Onuma, S. F. Chichibu, T. Sota, K. Asai, S. Sumiya, T. Shibata, and M. Tanaka, *Appl. Phys. Lett.* **81**, 652 (2002).

⁷J. Li, K. B. Nam, M. L. Nakarmi, J. Y. Lin, and H. X. Jiang, *Appl. Phys. Lett.* **81**, 3365 (2002).

⁸K. B. Nam, J. Li, M. L. Nakarmi, J. Y. Lin, and H. X. Jiang, *Appl. Phys. Lett.* **82**, 1694 (2003).

⁹K. B. Nam, M. L. Nakarmi, J. Li, J. Y. Lin, and H. X. Jiang, *Appl. Phys. Lett.* **83**, 878 (2003).

¹⁰J. Li, K. B. Nam, M. L. Nakarmi, J. Y. Lin, and H. X. Jiang, *Appl. Phys. Lett.* **83**, 5163 (2003).

¹¹E. Kuokstis, J. Zhang, Q. Fareed, J. W. Yang, G. Simin, M. Asif Kahn, R. Gaska, M. Shur, C. Rojo, and L. Schowalter, *Appl. Phys. Lett.* **81**, 2755 (2002).

¹²G. A. Slack, L. J. Schowalter, D. Morelli, and J. A. Freitas, Jr., *J. Cryst. Growth* **246**, 287 (2002).

¹³J. A. Freitas, Jr., G. C. B. Braga, E. Silveira, J. G. Tischler, and M. Fatemi, *Appl. Phys. Lett.* **83**, 2584 (2003).

¹⁴E. Silveira, J. A. Freitas, Jr., G. A. Slack, and L. J. Schowalter, *Phys. Status Solidi C* **0**, 2618 (2003).

¹⁵E. Silveira, J. A. Freitas, Jr., M. Kneissl, D. W. Treat, N. M. Johnson, G. A. Slack, and L. J. Schowalter, *Appl. Phys. Lett.* **84**, 3501 (2004).

¹⁶L. J. Schowalter, Y. Shusterman, R. Wang, I. Bhat, G. Arunmozhi, and G. A. Slack, *Appl. Phys. Lett.* **76**, 985 (2000).

¹⁷J. C. Rojo, L. J. Schowalter, R. Gaska, M. Shur, M. A. Khan, J. Yang, and D. D. Koleske, *J. Cryst. Growth* **240**, 508 (2002).

¹⁸H. Jiang, G. Y. Zhao, H. Ishikawa, T. Egawa, T. Jimbo and M. Umeno, *J. Appl. Phys.* **89**, 1046 (2001).

¹⁹B. V. Shanabrook, O. J. Glembocki, and W. T. Beard, *Phys. Rev. B* **35**, 2540 (1987).

²⁰W. J. Moore, J. A. Freitas, Jr., R. T. Holm, Yu. Melnik, and V. Dmitriev, *Appl. Phys. Lett.* (to be published).

²¹Q. Guo, M. Nishio, and H. Ogawa, *Phys. Rev. B* **64**, 113105 (2001).

²²J. J. Hopfield, *J. Phys. Chem. Solids* **15**, 97 (1960).

²³K. Kornitzer, T. Ebner, M. Grehl, K. Thonke, R. Sauer, C. Kirchner, V. Schwegler, M. Kamp, M. Leszczynski, I. Grezegory, and S. Porowski, *Phys. Status Solidi B* **216**, 5 (1999).

²⁴M. Suzuki, T. Uenoyama, and A. Yanase, *Phys. Rev. B* **52**, 8132 (1995).

²⁵A. F. da Silva and C. Persson, in *Optoelectronic Devices: III-V Nitride*, edited by M. Henini and M. Razeghi (Elsevier, New York, in press).